Unsteady open-channel flows over rough bed with and without emergent rigid vegetation: A laboratory experiment

J R Khuntia, Sébastien Proust, K K Khatua

Unsteady open-channel flows over rough bed with and without emergent rigid vegetation: A laboratory experiment

J. R. Khuntia
Ph.D. Scholar, Department of Civil Engineering, National Institute of Technology Rourkela, India & Visiting research scholar, Riverly, INRAE, Centre de Lyon-Villeurbanne, Villeurbanne, France

S. Proust
Researcher, Riverly, INRAE, Centre de Lyon-Villeurbanne, 5 rue de la Doua, Villeurbanne, France

K. K. Khatua
Professor, Department of Civil Engineering, National Institute of Technology Rourkela, India

ABSTRACT: We report here a laboratory study on the effects of bed roughness and emergent rigid vegetation on the unsteady flows associated with flash floods and extreme flood events. The flow structure of unsteady open-channel flows over rough bed with and without emergent rigid vegetation has been investigated in an 18m long and 3m wide laboratory flume. Steady uniform flows were also studied and served as reference flows. For both steady and unsteady flows, two geometries are tested: (1) uniform bed roughness (uniform dense synthetic grass modelling meadow) along the flume and (2) a uniform staggered distribution of emergent wooden circular cylinders (model of rigid vegetation) set on the bed roughness. Transient flow depths are simultaneously measured at six longitudinal positions using ultra-sonic sensors. Transient velocities are measured at one longitudinal position over the water column using a side looking ADV probe to estimate depth-averaged velocity. In order to compute ensemble averages of the flow parameters, 109 runs of the same hydrograph are carried out repeatedly at the flume entrance. Two consecutive runs are separated by a base flow. The ensemble averages of the measured discharge, flow depths and velocity are found to be converged after 72 runs. For the two geometries: at the peak flow of the hydrograph, the vertical profiles of mean streamwise velocity and horizontal Reynolds shear stress are comparable to the profiles obtained for steady uniform cases of same flow depth; and accelerated and decelerated velocity profiles are obtained during the rising limb and falling limb of the hydrograph, respectively. Reynolds shear stresses are also found to be higher during the rising limb than during the falling limb for a fixed flow depth. The hysteresis in the depth-averaged velocity / flow depth relationships is comparable in shape and size for the two geometries highlighting the weak effect of the rigid vegetation compared to the effects of un-stationarity.

1 INTRODUCTION

The study of unsteady open-channel flows is very important for assessing and predicting the flood hazard (flow depth, velocity, time of submersion) and to demarcate the area of inundation in the case of flash floods or floods in rivers of small and moderate size. What is specific to unsteady river flows is a hysteresis in the stage discharge curve, with a river flow conveyance higher during the rising water level than during the falling water level. The estimate of river flow conveyance under unsteady state is expected to be more complex in the presence of emergent vegetation (along floodplains, in the presence of riparian vegetation).

The importance of the study is to predict the complexity of the flow behavior due to unsteadiness under extreme flood events or flash floods. The combined effect of bed roughness and emergent rigid vegetation makes the flow process complicated in real field applications. So, the present laboratory study simplifies the real field case.

Over a rough bed, the vertical distribution of mean streamwise velocity is often approximated by a logarithmic law profile along a big part of boundary layer flows (Monin & Yaglom 1971). In the lower layer ($z/H < 0.3$) of shallow flows over rough surfaces found in rivers, bottom roughness may affect the development of the log-shaped velocity profile. Nikora and Smart (1997) found deviations from the log-law flow in the roughness layer ($z/H = 0.1$ to 0.3) which is a 3D inner layer of the flow in gravel-bed rivers. In such flows, a velocity inflection has been observed, resulting in so-called s-shaped profiles (Marchand, Jarrett & Jones 1984, Bathurst 1988, Ferro & Baiamonte 1994). Franca & Lemmin (2009) observed velocity profiles in two shallow gravel-bed rivers with low relative submergence. The log-shaped profiles and S-shaped profiles were simultaneously observed in these flows indicating the possibility of 3D flow inside the roughness layer ($k/H >\approx 0.6$, where k is the equivalent sand grain size of the bed roughness and H is the flow depth). Bombar, Güney, Tayfur & Elçi (2010) computed the mean velocities and turbulence intensities with 15 runs of the same triangular shape hydrograph, based on laboratory experiments. The experiments were conducted in a rectangular flume (18m × 0.7m × 05m) with a bed slope of 0.004. The bed of the flume was composed of nonuniform sediment mixture with $d_{50} = 0.43$ and thickness was 20mm. The mean velocities and turbulence intensities were found larger in the rising limb of the hydrograph as compared to the falling limb for the same flow depth. Alfadhli, Yang & Sivakumar (2013) investigated the vertical profiles of longitudinal mean velocity in steady and unsteady non-uniform open channel flows. It was found that for steady/unsteady flow the Log law is applicable only in the inner region ($z/H < 0.2$) when compared with the measured longitudinal velocity. Dupuis, Proust, Berni & Paquier (2016) experimentally investigated steady open-channel flows subjected to a longitudinal transition in hydraulic roughness, from bed friction to emergent cylinder drag and vice versa. The vertical profiles of longitudinal mean velocity in the cylinder alignment, the velocity bulge and constant velocity region were clearly observed in the near-bed region at $z/D = 1.9$ and at $z/D = 4.1$ respectively (where D is the diameter of cylinder). Tognin, Peruzzo, De Serio & et al. (2019) studied the propagation of a solitary wave in the presence of emerging rigid cylinders mimicking the propagation of tsunamis through mangrove forests. Specifically, it was observed that the vegetation reduces the wave height proportionally to the vegetation density. During base flow conditions, the vertical profile of longitudinal velocity clearly showed a logarithmic profile in bare soil condition, whereas it turned into a rather uniform velocity distribution in the presence of vegetation.

In the literature, the separated and combined effects of a rough bed and emergent rigid vegetation on unsteady flow parameters (mean velocity and turbulence statistics) has not been studied so far, to the authors' knowledge. The present study therefore focuses on these issues. A particular attention was paid to the convergence of flow parameters based on ensemble averages: (1) to confirm the mean velocity profiles and Reynolds shear stress for unsteady accelerated, and decelerated flows over a rough bed; and (2) to study the vertical distribution of mean flow and Reynolds shear stress for unsteady accelerated and decelerated over a rough bed with emergent rigid vegetation.

2 EXPERIMENTAL SETUP AND PROCEDURES

2.1 *Flume and measuring devices*

The experiments have been conducted in a rectangular open-channel flume (18 m long and 3 m wide) in the Hydraulics and Hydro-morphology laboratory of the RiverLy research Unit of INRAE Lyon-Villeurbanne, France (Figs. 1 to 3). The longitudinal bed slope of the flume is $S_0 = 1.05\times10^{-3}$ m/m. Because of some laboratory constraints, the experiments are performed in the left-hand part of the flume, using 1/3 of the total flume width (working width = 1 m, working length = 18 m). A vertical Plexiglas sidewall is used to isolate a 1 m-wide open-channel on the left-hand side of the flume. Figure 2a shows the side views of the channel with a rough bed only (M = Meadow) and with emergent circular cylinders set on the rough bed (W = Woodland), and Figure 2b shows top views of the array of cylinders and elementary pattern of cylinders with the ADV probe position for velocity measurements. Figure 3 shows the channel view of the two

configurations studied (W and M). The 1m wide open-channel is supplied by a 1 m wide inlet tank, the inflow being monitored using a flow meter (Water flux) at an acquisition rate of 50 Hz. The glass bed has been covered by: a) artificial dense grass (M); b) a staggered distribution of wooden circular cylinders set on the artificial grass (W). The Manning's roughness coefficient n of the rough bed surface is 0.0157 s/m$^{1/3}$. A Cartesian right-handed coordinate system is used in which x-, y-, and z-axes are aligned with the longitudinal (parallel to the flume bottom), transverse, and vertical (normal to the flume bottom). The water surface elevations are measured with six ultrasonic sensors (BAUMER UNDK 20I6912/S35A) located at longitudinal positions x = 3 m, 6 m, 10 m, 13 m, 15 m and 17 m. At each measuring point, elevation is recorded at a rate of 50 Hz with an accuracy better than0.3 mm. Velocities are measured over the water column at x = 13m, using a side-looking ADV probe (Vectrino plus, Nortek) with a sampling rate of 100 Hz and an accuracy of 0.5% of the measured velocity. The measurement is taken at one fixed position (x = 13m) for the two configurations M and W.

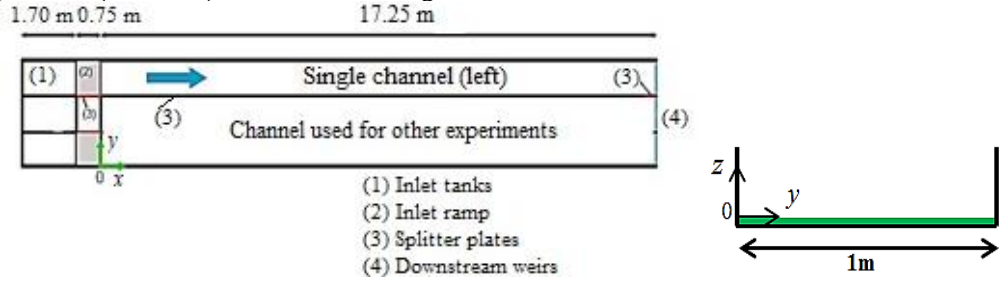

Figure 1. Schematic top view and cross-sectional view of the open-channel (using 1/3 of the total flume width), INRAE, Lyon

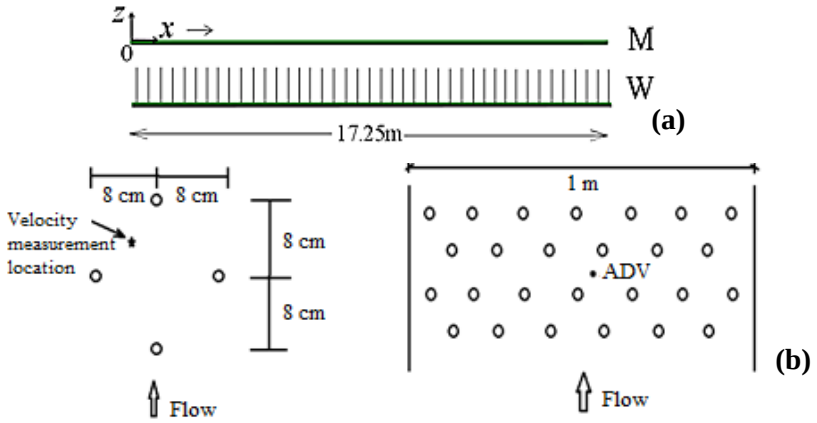

Figure 2. (a) Side view of the channel with rough bed (M = Meadow) and array of emergent rigid cylinders (W = woodland) placed on the rough bed. (b) Top views of the cylinder distribution, indicating the location of the velocity measurement using the ADV probe

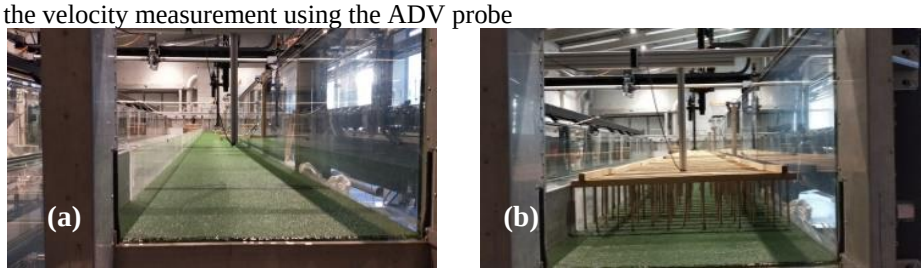

Figure 3. (a) Uniform rough bed (dense artificial grass modeling meadow), picture from downstream. (b) Uniform distribution of emergent cylinders placed on the artificial grass (model of a woodland)

2.2 *Flow conditions*

One hundred nine identical runs of the same hydrograph are carried out at the flume entrance in order to make ensemble averaging of the flow variables (water elevation and velocity). Each hydrograph is composed of a steady base flow (flow depth h_b), a linear rising limb until the peak

water depth h_p and a falling limb until the next base flow (Fig. 4). The associated unsteadiness flow parameter λ (Eq. 1, where T_r is the duration of the rising limb and S_o is the longitudinal slope of the bed) equals to 0.65 (same order of magnitude of hydrographs as those carried out by Lai, Liu & Lin (2000). The unsteadiness parameter λ represents the ratio of the rising speed of water surface to the wave speed at the peak flow.

$$\lambda = \frac{h_p - h_b}{S_o T_r \sqrt{g h_p}} \quad (1)$$

Due to software constraints, four sequences of twenty four runs are launched (Fig. 4a), and eventually a sequence of 13 runs. At each measuring point, the 109 runs are carried out without switching off the pump to ensure the repeatability of the process.

2.3 *Unsteady data treatment*

First, both instantaneous values of water level and velocity are filtered. Water level measurements are despiked. The ADV velocity data are filtered based on the values of the signal to noise ratio (SNR) and signal correlation (COR). The velocity data with a SNR lower than 22dB and a COR lower than 85% are removed from the time series. To account for a small misalignment of the ADV probe with the longitudinal direction, corrections of transverse velocity data are carried out based on Peltier et al. (2013).

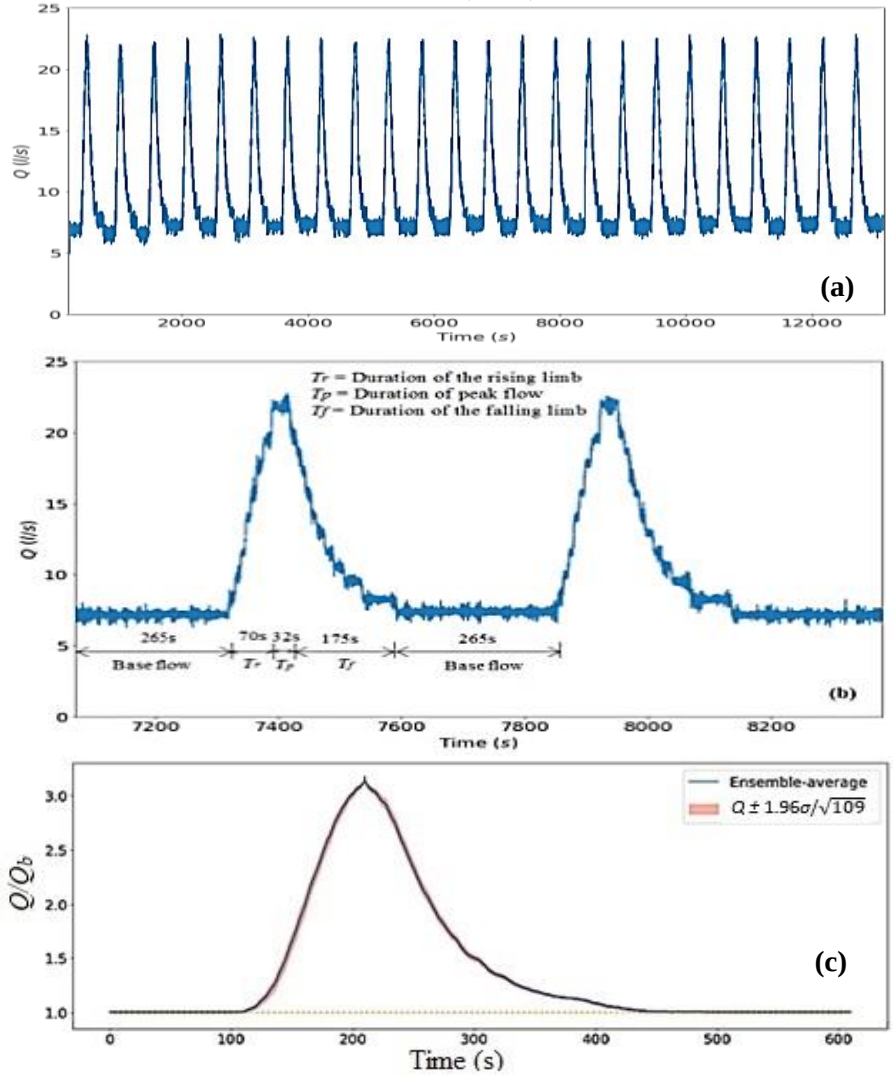

Figure 4: (a) Times series of inlet flow rate Q during 24 hydrograph runs. (b) Time series of Q during two consecutive runs, highlighting the different time periods. (c) Ensemble average of $Q\ (t)$ for the 109 runs [Q is normalized by base flow Q_b].

Second, to perform ensemble averaging of water depth and velocity data, a windowing of instantaneous data is carried out by (1) detecting the peak discharge value of instantaneous flow rate *Q (t)* and (2) considering a window centered on the detected peak value. The window width is chosen to include the base flow (i.e., 7 *l*/s) before and after the hydrograph, and the rising and falling limbs (Fig. 4b).

Third, an ensemble averaging of the 109 runs is computed (Fig. 4c). If *P(t)* is the instantaneous value of a flow parameter *P*, the ensemble average $< P(t) >$ and the associated standard deviation are defined by

$$< P(t) >= \frac{1}{109}\sum_{i=1}^{109} P_i(t) \quad (2)$$

$$\sigma(t) = \sqrt{\frac{1}{109}\sum_{i=1}^{109}(P_i(t) - < P(t) >)^2} \quad (3)$$

Note that, a 5 second moving time average is used to smoothen the flow parameters.

3 EXPERIMENTAL RESULTS

3.1 *Convergence of the flow parameters*

We denote Q_{final}, H_{final} and U_{xfinal} as the ensemble averages of discharge *Q*, flow depth *H*, and local longitudinal velocity U_x, respectively, using the 109 runs. Figure 5 shows the convergence of *Q*, *H* and U_x as a function of the number of runs.

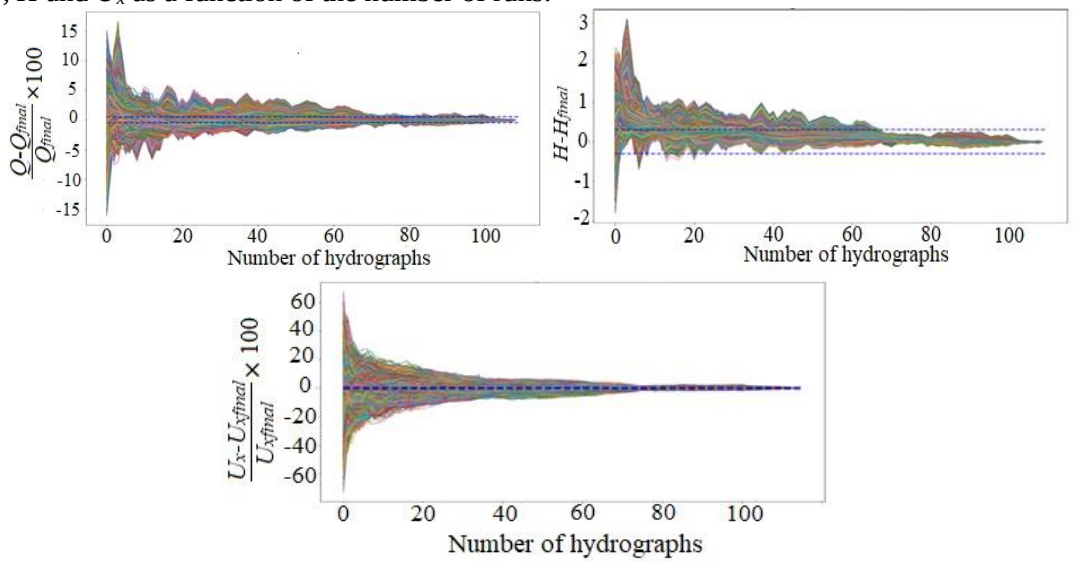

Figure 5: Convergence of the ensemble averages of discharge *Q*, flow depth *H*, and local velocity U_x at elevation of z = 24mm from bed roughness. The dashed lines bound measurement accuracy.

The convergence of the ensemble averages of discharge *Q*, flow depth *H*, and local streamwise velocity U_x was obtained after 45 runs, 50 runs, and 72 runs, respectively.

3.2 *Mean streamwise velocity profiles*

The vertical profiles of streamwise velocity U_x are found to be superimposed when comparing with the steady uniform flow case and the base flows of same discharge at 7 *l*/s. This is happening for both the geometries studied (Fig. 6a, b) (i.e., uniform meadow M, uniform woodland W). It is seen in section 3.1 that after 72 repetitions of the same hydrograph, the ensemble average of the velocity become converged. For both the two configurations of the fixed flow (i.e., 15 *l*/s), and for both the accelerated and decelerated longitudinal velocity profiles are deviating from the uniform flow cases (Fig. 6c, d). A constant velocity region was observed in case of emergent rigid vegetation (Fig. 6d). Higher values are found during the rising cases as compared to that during the falling limb cases. The longitudinal velocity profiles of steady uniform flow case are found to be very similar to the peak flow (i.e., 22 *l*/s) of the unsteady case for the both configurations studies (Fig. 6e, f).

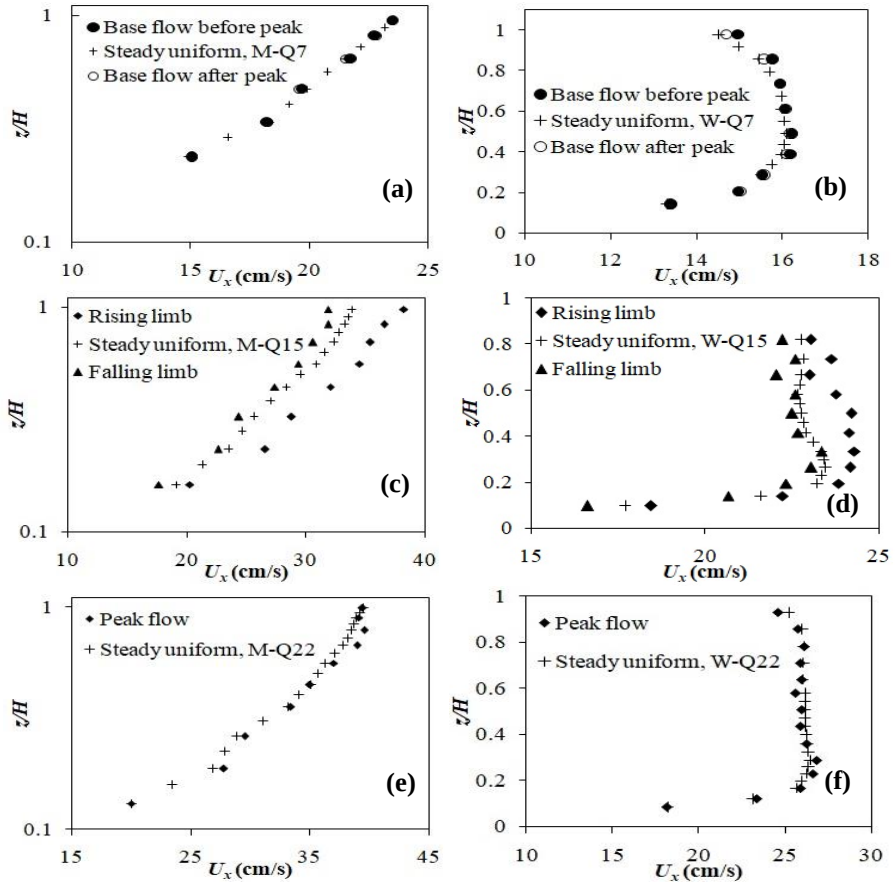

Figure 6: Vertical distribution of streamwise velocity U_x for a steady uniform flow and at base flows of 7 *l*/s for (a) a uniform Meadow (M) and (b) a uniform Woodland placed over the meadow (W), at a fixed flow of 15 *l*/s for rising limb and falling limb, and steady uniform flow of 15 *l*/s for (c) a uniform Meadow (M) and (d) a uniform Woodland placed over the meadow (W) at the peak of the hydrograph (22 *l*/s) and for a steady uniform flow of 22 *l*/s (e) Uniform Meadow (M) (f) Uniform Wood (W)

3.3 *Reynolds shear stress profiles*

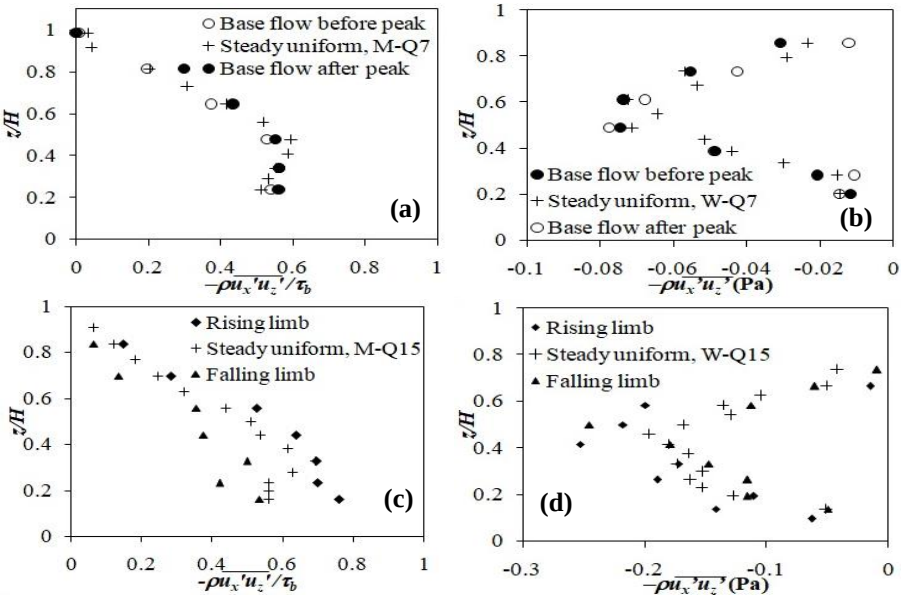

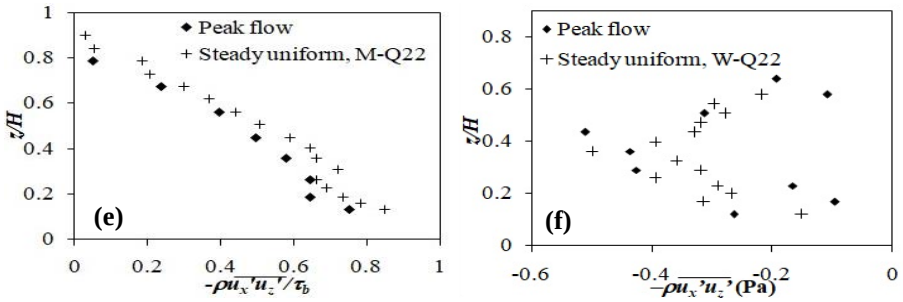

Figure 7: Reynolds shear stress profiles for a steady uniform flow and at base flows of 7 *l*/s for (a) a uniform Meadow (M) and (b) a uniform Woodland placed over the meadow (W), at an intermediate flow of 15 *l*/s for rising limb and falling limb, and steady uniform flow of 15 *l*/s for (c) a uniform Meadow (M) and (d) a uniform Woodland placed over the meadow (W), at the peak of the hydrograph and for a steady uniform flow of 22 *l*/s (e) Uniform Meadow (M) (f) Uniform Wood (W)

The vertical profiles of Reynolds shear stress are found to be superimposed when comparing with the steady uniform flow case and the base flows of the same discharge i.e. at 7 *l*/s. This is valid for the both the geometries studied (Fig. 7a, b) (i.e., uniform meadow M, uniform woodland W). For these two configurations, at a fix flow of 15 *l*/s, both the accelerated and decelerated Reynolds shear stresses are found to be deviating from the results of uniform flow cases. Higher values are found to be occurring during the rising limb cases as compared to those values during the falling limb cases (Fig. 7c, d). The Reynolds shear stresses of the steady uniform flow cases are also found to be very similar to the peak flow of unsteady cases for the both configurations studies (Fig. 7e, f).

3.4 *Hysteresis loops*

Figure 8 shows the clockwise hysteresis loops in the depth-averaged longitudinal velocity / flow depth for both uniform meadow M and uniform woodland W configurations. For both geometries, given a flow depth value, the flow conveyance is higher during the rising limb than during the falling limb. More surprisingly, the extents of both loops are very similar, highlighting that there is very weak effect of the emergent rigid vegetation on the transient features of the flows.

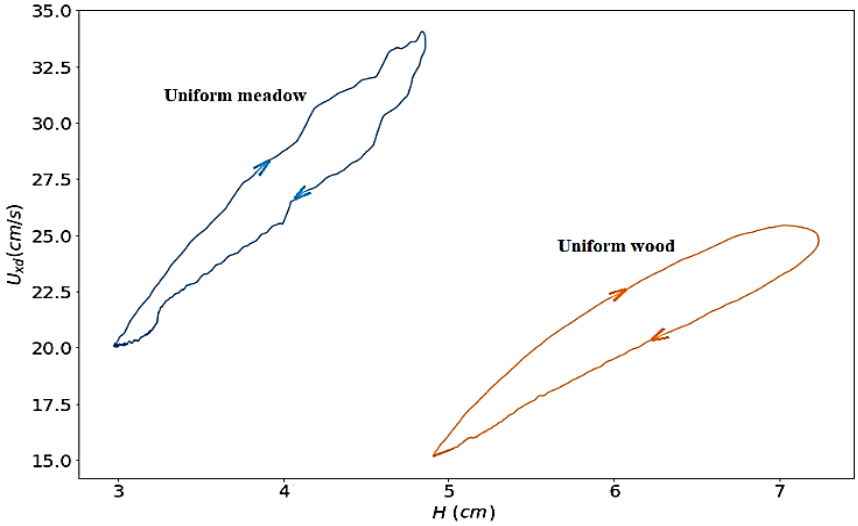

Figure 8: Hysteresis loops of depth averaged velocity U_{xd} against flow depth H for a channel bed with a uniform meadow (M) and a uniform woodland placed over the meadow (W)

4 CONCLUSIONS

- An experimental investigation on unsteady flows over rough bed, with and without emergent rigid vegetation has been carried out in a laboratory flume. The ensemble averages of inlet

flow discharge, local streamwise velocity and flow depth are found to be converged after 72 runs of the same hydrograph.

- Over the rough bed with emergent rigid vegetation (configuration W) and without (configuration M), the vertical profiles of local mean velocity and Reynolds shear stress (when ensemble averaged) for the base flows of the hydrographs and the steady uniform flow of same discharge are found to be superimposed, as expected.
- At a fixed intermediate flow, accelerated (during the rising limb) and decelerated (during the falling limb) mean velocity profiles and Reynolds shear stress profiles are deviating from the steady-uniform flow case conditions. Higher values are found during the rising limb than during the falling limb for both geometries (W and M) studied.
- The velocity profiles and Reynolds shear stress profiles at the peak flow of the hydrograph are found to be very similar to the ones for a steady uniform flow cases for both geometries W and M.
- The hysteresis loops in the depth-averaged velocity / flow depth relationships for the two geometries have the same shape and dimension, highlighting that rigid emergent vegetation has no damping effect on the non-stationary features of the studied flows.

5 ACKNOWLEDGEMENT

- Authors wish to thank CEFIPRA/IFCPAR for sanctioning Raman-Charpak Fellow 2018-2019, Sanction No: SANCTION NO. FT/092/18-19, Reference No. IFC/RCF/2019/1754 to the first author to conduct experimental research on “unsteady flow in rough open channels” at Hydraulics and Hydro-morphology laboratory (HHLab.) of the RiverLy research unit of INRAE (Formerly IRSTEA), Centre de Lyon-Villeurbanne, France.

REFERENCES

Alfadhli, I., Yang, S., & Sivakumar, M., 2013. Velocity distribution in non-uniform/unsteady flows and the validity of log law. *SGEM 2013: 13th International Multidisciplinary Scientific Geoconference* (pp. 425-432). Bulgaria: SGEM.

Bathurst, J. C., 1988. Velocity profile in high-gradient, boulder-bed channels, *Proc. Int. Conf. on Fluvial Hydraulics IAHR*, 29-34, Budapest, Hungary.

Bombar, G., Güney, M. Ş., Tayfur, G., & Elçi, Ş., 2010. Calculation of the time-varying mean velocity by different methods and determination of the turbulence intensities. *Scientific Research and Essays*, *5*(6): 572–581.

Dupuis, V., Proust, S., Berni, C., & Paquier, A., 2016. Combined effects of bed friction and emergent cylinder drag in open channel flow. *Environmental Fluid Mechanics*.

Ferro, V., & Baiamonte, G., 1994. Flow velocity profiles in gravel-bed rivers. *Journal of* Hydraulic *Engineering*, *120*(1): 60-80.

Franca, M. J., & Lemmin, U., 2009. The simultaneous occurrence of logarithmic and S-shaped velocity profiles in gravel-bed river flows. *Archives of Hydro-Engineering and Env.Mechanics*, *56*(1-2), 29-41.

Lai, C.J., Liu, C.L. and Lin, Y.Z., 2000. Experiments on flood-wave propagation in compound channel. *Journal of Hydraulic Engineering*, *126*(7): 492-501.

Marchand, J. P., Jarrett, R. D., & Jones, L. L., 1984. *Velocity profile, water-surface slope, and bed-material size for selected streams in Colorado*. US Department of the Interior, Geological Survey open file report, 84-733.

Monin, A. S. and Yaglom, A. M., 1971. Statistical Fluid Mechanics: Mechanics of turbulence, vol. 1, The MIT Press, Cambridge, Massachusetts, USA.

Nikora, V. I., & Smart, G. M., 1997. Turbulence characteristics of New Zealand gravel-bed rivers. *Journal of Hydraulic Engineering*, *123*(9): 764-773.

Peltier, Y., Rivière, N., Proust, S., Mignot, E., Paquier, A. and Shiono, K., 2013. Estimation of the error on the mean velocity and on the Reynolds stress due to a misoriented ADV probe in the horizontal plane: Case of experiments in a compound open-channel. *Flow Measurement and Instrumentation*, *34*: 34-41.

Tognin, D., Peruzzo, P., De Serio, F., Ben Meftah, M., Carniello, L., Defina, A., & Mossa, M., 2019. Experimental Setup and Measuring System to Study Solitary Wave Interaction with Rigid Emergent Vegetation. *Sensors*, *19*(8): 1787.